1   **RNase III-independent autogenous regulation of *Escherichia coli* polynucleotide phosphorylase**

2   ***via* translational repression**

3

4   Thomas Carzaniga[1,2], Gianni Dehò[1], Federica Briani[1*]

5

6   [1]Dipartimento di Bioscienze, Università degli Studi di Milano, Milan, Italy

7   [2] Present address: BioMeTra, Università degli Studi di Milano, Milan, Italy

8

9

10   [*]Corresponding author. Mailing address:

11   Dipartimento di Bioscienze

12   Università degli Studi di Milano

13   Via Celoria 26 / A4

14   20133 Milano

15   Phone: (+39)02.5031.5033

16   Fax: (+39)02.5031.5044

17   E-mail: federica.briani@unimi.it

18

19   **Running title:** Autoregulation of *E. coli* PNPase

20   **Keywords:** PNPase, post-transcriptional regulation; translation repressor; RNA decay; RNase E

21

STRUCTURED SUMMARY

ABSTRACT

22

23

24 The complex post-transcriptional regulation mechanism of *Escherichia coli pnp* gene, which encodes

25 the phosphorolytic exoribonuclease polynucleotide phosphorylase (PNPase), involves two

26 endoribonucleases, namely RNase III and RNase E, and PNPase itself, which thus autoregulates its

27 own expression. The models proposed for *pnp* autoregulation posit that the target of PNPase is a

28 mature *pnp* mRNA previously processed at its 5'-end by RNase III, rather than the primary *pnp*

29 transcript (RNase III-dependent models) and that PNPase activity eventually leads to *pnp* mRNA

30 degradation by RNase E. However, some published data suggest that *pnp* expression may also be

31 regulated through a PNPase-dependent, RNase III-independent mechanism. To address this issue, we

32 constructed isogenic $\Delta pnp\ rnc^+$ and $\Delta pnp\ \Delta rnc$ strains with a chromosomal *pnp-lacZ* translational

33 fusion and measured β-galactosidase activity in the absence and presence of PNPase expressed by a

34 plasmid. Our results show that PNPase also regulates its own expression *via* a reversible RNase III-

35 independent pathway acting upstream of the RNase III-dependent branch. This pathway requires the

36 PNPase RNA binding domains KH and S1, but not its phosphorolytic activity. We suggest that the

37 RNase III-independent autoregulation of PNPase occurs at the level of translational repression,

38 possibly by competition for *pnp* primary transcript between PNPase and the ribosomal protein S1.

39

IMPORTANCE

41 In *Escherichia coli* polynucleotide phosphorylase (PNPase, encoded by *pnp*) post-transcriptionally

42 regulates its own expression. The two models proposed so far posit a two-step mechanism in which

43 RNase III, by cutting the leader region of the *pnp* primary transcript, creates the substrate for PNPase

44 regulatory activity, eventually leading to *pnp* mRNA degradation by RNase E. In this work we provide

45 evidence supporting an additional pathway for PNPase autogenous regulation in which PNPase acts as

46 a translational repressor independently of RNase III cleavage. Our data give a new contribution to the

47 understanding of the regulatory mechanism of *pnp* mRNA, a process long since considered a

48 paradigmatic example of post-transcriptional regulation at the level of mRNA stability.

49

50

51

INTRODUCTION

A wealth of mechanisms that control gene expression and an intricate network of regulatory interactions subtly and promptly adapt the presence and concentration of gene products to a variety of environmental and developmental conditions. Autogenous regulation of *pnp* gene in *Escherichia coli* has long since considered an example of regulation at the level of mRNA stability. This gene codes for polynucleotide phosphorylase (PNPase), a phosphorolytic 3'-5' exoribonuclease and a template-independent NDP-dependent RNA polymerase conserved in bacteria and eukaryotic organelles (1, 2). *E. coli* PNPase plays a major role in RNA turnover and metabolism (3) and has been implicated in several processes such as adaptation and growth in the cold, biofilm formation, response to oxidative stress and DNA damage (4-8).

Early studies showed that *pnp* belongs to two overlapped operons transcribed from P1 (upstream of *rpsO*) and P2 (upstream of *pnp*) promoters (9-12). Both *pnp*-encoding mRNAs generated from P1 and P2 are efficiently processed by RNase III at a hairpin in the *pnp* untranslated leader region (UTR) between P2 and *pnp* UUG start codon (Fig. 1). In the absence of RNase III, the primary transcripts are stable and efficiently translated, whereas upon RNase III processing *pnp* mRNA is rapidly degraded and PNPase production ceases (13, 14). However, in the absence of PNPase both RNase III-processed and unprocessed *pnp* mRNAs are stable (15). These observations led to the conclusion that PNPase regulates its own expression in an RNase III-dependent (RTD) manner.

Two basic alternative models have been proposed by Portier and co-workers to explain how PNPase regulates its own expression upon RNase III cleavage. A former model (15) essentially postulated that PNPase could act as a translational repressor by binding determinants (translational operator) in the 5'-UTR of the RNase III-processed *pnp* mRNA, thus promoting degradation of the untranslated mRNA by RNases other than PNPase. On the contrary, in the primary transcript the translational operator could not be available to PNPase; as a consequence, the *pnp* mRNA could be translated and thus stabilized. This model was supported by the observation that mRNA stability of a *pnp-lacZ* translational fusion inversely correlated with ectopically expressed PNPase abundance whereas it decreased in the presence of mutations affecting its translation efficiency (15).

A later model (16) was based on the observation that RNase III double-strand cut generates a processed mRNA with a double stranded stem in which the 5'-monophosphate recessed end is protected by the dangling 3'-end of a short RNA. It was then proposed that the processed mRNA with a 5'-end duplex would maintain the stability and translatability properties of the primary transcript; on

84   the other hand, PNPase could bind such a structure and degrade the short upstream strand of the

85   duplex, thus releasing a stem-less processed *pnp* mRNA. The *pnp* mRNA devoid of its 5'-end hairpin

86   would become unstable and poorly, if at all, translatable, regardless of the intracellular PNPase

87   concentration, as shown *in vivo* by these authors. In both models autogenous regulation is exerted

88   downstream of the RNase III cleavage step and leads, eventually, to *pnp* mRNA instability.

89   Within this framework we previously showed that the RNase III-processed *pnp* mRNA devoid of

90   the RNase III hairpin at its 5'-end is not translatable and is degraded by RNase E in a PNPase-

91   independent manner (17). It thus appears that, upon RNase III cleavage, PNPase simply degrades the

92   short 5'-complementary strand and is not further implicated in PNPase mRNA instability or

93   translational repression. However, some previously published data may lend some support to a

94   PNPase-dependent, RNase III-independent (RTI) regulatory mechanism, as well as translational

95   repression by PNPase (see Discussion) (14, 15).

96   In this work, we provide evidence that PNPase also regulates its own expression *via* an RTI

97   pathway. This pathway requires the PNPase RNA binding domains KH and S1 but not its

98   phosphorolytic activity and operates upstream of the RTD pathway. We suggest that the RTI

99   autoregulation of PNPase occurs at the level of translational repression, possibly by competition

100   between PNPase and the ribosomal protein S1 for the *pnp* mRNA.

101

102

103   **MATERIALS AND METHODS**

104

105   **Bacterial strains and plasmids**. Bacteria, plasmids, and phage are described in Table 1 with a brief

106   outline of their construction by standard techniques. Unless otherwise stated, bacterial cultures were

107   grown at 37 °C in LD medium (18) supplemented as indicated. When indicated, 2 g/l arabinose, 2 g/l

108   glucose, 50 μg/ml ampicillin, and 30 μg/ml chloramphenicol were added.

109

110   **Enzymes and reagents**. Wild type PNPase purification and α-PNPase polyclonal antibodies have been

111   previously described (19, 20). Purified ribosomal protein S1 and α-S1 antibodies were a generous gift

112   of Udo Bläsi.

113

114   **PNPase autoregulation and RNA-binding assays**. Bacterial strains harbouring λGF2 prophage (*pnp-*

115   *lacZ* translational fusion) and pBAD24 derivatives expressing the different *pnp* alleles under *araBp*

116   promoter were grown over night at 37 °C in 5 ml LD glucose (*pnp* repressed) and 0.5 ml of the culture

117   was centrifuged 30 seconds at RT, resuspended in an equal volume of LD, and diluted 200 fold in 40

118   ml LD broth with glucose (*pnp* repressed) or arabinose (*pnp* expressed) at 37 °C. The cultures were

119   further incubated with shaking at 37 °C up to OD600 = 0.8; 10 ml samples were collected by

120   centrifugation, resuspended in 0.5 ml TEDP (0.1 M Tris HCl, 1 mM EDTA, 1 mM DTT and 1 mM

121   PMSF protease inhibitor) and disrupted by sonication (2x30 s pulses at 40% amplitude). The samples

122   were centrifuged 15 minutes at 12,000 rpm at 4 °C to remove cell debris. Protein concentration in the

123   crude extracts was determined by the Coomassie (Bradford) protein assay kit (THERMO Scientific). β-

124   galactosidase activity of the extracts was measured as described (Miller, 1992). Specific activity was

125   expressed as nmoles of *ortho*-nitrophenyl-β-D-galactopyranoside (ONPG) converted to *ortho*-

126   nitrophenol min^{-1} mg of protein^{-1}. The PNPase content of the samples was evaluated by western

127   blotting 400 ng total proteins samples using α-PNPase antibodies (21) and densitometric analysis of the

128   film using ImageQuant software (Molecular Dynamics). Electrophoretic Mobility Shift Assays

129   (EMSA) were performed as described (19). PNPase-RNA crosslinking assays were performed by

130   incubating 100,000 cpm of the [α-^{32}P]-CTP uniformly labeled RNA probes shown in Fig. 1 for 20 min

131   at 21°C in Binding Buffer (50 mM Tris-HCl at pH 7.4, 50 mM NaCl, 0.5 mM DTT, 0.025% NP40

132   [Fluka] and 10% glycerol) with either 400 ng of crude extract or purified proteins in a final volume of

133   10 μl. The samples were UV-irradiated (254 nm, 2.8 J/cm^2), treated with RNase A and the cross-linked

134   proteins were fractionated by 10% SDS-PAGE and analyzed by phosphorimaging (21). RNA probes

135   were obtained by T7 RNA polymerase transcription of DNA templates produced by PCR with primers

136   listed in Table 2 and plasmid pAZ101 as a template.

137

138

139   **S1-PNPase binding assay.** *Crude extract preparation.* 50 ml of exponential cultures (OD_{600}=0.8) of C-

140   1a/pAZ101and C-1a/pAZ133 were collected by centrifugation, resuspended in 0.35 ml Buffer A

141   (10mM Tris–HCl, pH 7.5, 100 mM NaCl, 10 mM MgCl2) and lysed by freeze thawing with 0.4 mg/ml

142   lysozyme. 0.25 ml Buffer A supplemented with 0.05% Tween and 0.1 U/μl DNase I (Promega) were

143   then added. After 20 min on ice, the extracts were centrifuged at 13200 rpm for 10 min at 4 °C. The

144   absorbance at 260 nm was measured to get a rough estimate of crude extract concentration (22,

145   23).When indicated, the extracts were incubated 20 min at 37 °C with 250 ng/μl RNase A. *S1 coating*

146   *of the beads and analysis of S1-PNPase binding.* His-tagged S1 was purified with Ni-NTA agarose

147   (Qiagen) following the manufacturer's protocol from an exponential culture of C1a/pREP4, pQE31-S1

148   (21) induced with 1 μM IPTG. 25 μl of Ni-NTA agarose beads (Qiagen) were washed with buffer A

149   and incubated 1 hour at 4 °C in a rotatory device with 150 pmol His-tagged S1 in 400 μl 10 mM Tris–

150   HCl, pH 7.5, 300 mM NaCl, 15 mM imidazole, 0.005% Tween. S1-coated beads were incubated 1 hour

151   at 4 °C in a rotatory device with 2-4 OD_{260} of crude extracts diluted in Buffer B (10 mM Tris–HCl, pH

152   7.5, 280 mM NaCl, 20 mM imidazole; final volume, 500 μl). After incubation, the beads were washed

153   twice with 500 μl Buffer B. S1 was eluted by incubating the beads in 40 μl Buffer C (10 mM Tris–HCl,

154   pH 7.5, 30 mM NaCl, 250 mM imidazole). Proteins were run on 10% SDS-PAGE and the gels were

155   either silver stained with the SilverQuest Silver Staining kit (Invitrogen) or blotted onto a nitrocellulose

156   (Hybond C) sheet and incubated with polyclonal anti-PNPase antibodies (20).

157

158

RESULTS

RNase III-independent autogenous regulation of PNPase

To monitor *pnp* operon regulation by PNPase we used a previously described reporter system consisting of a translational fusion between the 5' region of the *rpsO-pnp* operon including the first 61 codons of *pnp* (Fig. 1) and the reporter gene *lacZ* carried by the transducing λGF2 phage (14, 24, 25). Single Δ*pnp* and double Δ*pnp* Δ*rnc* mutants were lysogenized with λGF2 and transformed by pBAD24 plasmid vector derivatives harbouring *pnp* (or *pnp* mutants as described below) under control of the arabinose-inducible promoter *araBp*. PNPase was expressed in the presence of arabinose (which induces transcription from *araBp*), whereas in the presence of glucose (*araBp* repression), as well as in the strains harbouring the empty vector in either conditions, no PNPase could be detected by western blotting (data not shown).

Repression exerted by PNPase on the expression of the reporter *lacZ* was expressed as the ratio of β-galactosidase specific activity in the presence of glucose to that in the presence of arabinose. As shown in Fig. 2, induction of wild type PNPase exerted, as expected, approximately 6 fold repression of β-galactosidase in the *rnc*[+] strain. In the Δ*rnc* mutant, however, repression was reduced to about 3 to 4 fold, but not abrogated as it would be predicted by the current autoregulation model. This result is consistent with data obtained by Portier and collaborators (14) in a different *E. coli* strain and with a similar system. It thus appears that PNPase participates in an RNase III independent (RTI) mechanism of regulation of *pnp* operon expression.

RNase III-independent autogenous regulation requires RNA binding but not phosphorolytic activity

To test whether this residual, RNase III-independent autogenous regulation required phosphorolytic, RNA binding, or both PNPase activities, we measured post-transcriptional repression levels by PNPase mutants affected in either activity, namely Pnp-ΔKHS1, which is missing the two RNA binding domains (24, 26), and Pnp-S438A, which is devoid of phosphorolytic activity (19). To test whether the mutant retained RNA binding activity, we performed RNA-PNPase cross-linking experiments, as previously described (21). As shown in Fig. 3A, the ratio of PNPase-bound RNA to PNPase, normalized to the wild type PNPase signals, was not affected by the S438A mutation, whereas Pnp-ΔKHS1 exhibited reduced RNA binding activity, as previously described (27).

190   Autogenous regulation by *pnp-ΔKHS1* mutant was severely impaired in both *rnc*[+] (as previously

191   shown; 24, 25, 27) and *rnc*[-] strains (Fig. 2). On the contrary, the *pnp-S438A* mutation only partially

192   reduced repression in either strain. Namely, in *rnc*[+] the repression factor was 2.61 fold (about the half

193   of maximum repression attained by wild type PNPase in the *rnc*[+] strain) and 2.68 in *rnc*[-] background

194   (about 74% of wild type PNPase repression in the same background).

195   Overall these data suggest i) that PNPase acts as a repressor of its own expression on the native

196   (not processed by RNase III) *pnp* transcript and ii) that PNPase phosphorolytic activity is dispensable

197   for RTI regulation. Thus this mechanism acts upstream and in addition to the control of *pnp* mRNA

198   stability exerted on RNase III-processed mRNA. Since it has been shown that, in the absence of RNase

199   III, stability of *pnp* mRNA is not affected by PNPase (15), such an RTI regulation of *pnp* operon

200   expression should depend on translational repression by PNPase.

201   It should be mentioned that although in our system the genes encoding the wild type and mutant

202   PNPases cloned under the *araBp* promoter lack the 5'-UTR regulatory regions, the PNPase

203   intracellular concentration in the arabinose-induced cultures was higher for the mutants than for the

204   wild type, both in the *rnc*[+] and the *rnc*[-] strains (Fig. 3A). This could probably depend on the higher

205   copy number of the ColE1-type vector expressing mutant PNPases (28). However, in spite of higher

206   level of Pnp-ΔKHS1, the RTI pathway was impaired in the strain complemented by *pnp-ΔKHS1* thus

207   further supporting the key role of PNPase RNA binding domains in the RTI mechanism.

208

209   **PNPase and ribosomal protein S1 competitive binding to the *pnp* mRNA leader sequence**

210   We previously showed by UV cross linking experiments that both PNPase and ribosomal protein S1

211   bind to the *pnp* mRNA leader region RNA and modulate the stability of this messenger (21). It is thus

212   conceivable that PNPase may prevent translation by competing with S1 (and/or the 30S ribosomal

213   subunit) for binding to specific sites. Alternatively, PNPase could interact with S1 and form a complex

214   that binds to *pnp* mRNA and interferes with its translation. The latter hypothesis, however, was not

215   supported by the observation that in an *E. coli* crude extract S1-coated beads were able to capture wild

216   type PNPase but not the ΔKHS1 mutant enzyme (Fig. 3B). Moreover, if the extract was pretreated with

217   RNase A to destroy RNA, wild type PNPase-S1 interaction was no longer detectable (Fig. 3B); this

218   suggests that S1 and PNPase are tethered by RNA rather than directly interact with each other.

219   To test the former hypothesis, *i. e.* PNPase-S1 competition for *pnp* mRNA leader region, we performed

220   competitive RNA-protein cross linking by adding increasing concentrations of PNPase to the PNPA157

221   RNA probe, which extends 157 nt from *pnp-p2* promoter and covers the 5'-UTR and the translation

222   initiation region (TIR; Fig. 1), incubated with S1. As shown in Fig. 4A, 9-12 nM PNPase is sufficient

223   to displace S1 protein (30 nM; half saturation) from the RNA probe . Moreover, the affinity of

224   PNPA157 RNA probe with PNPase, as measured by EMSA, was much stronger than that with S1 (Kd

225   = 1.8 and 65 nM, respectively; Fig. 4B). In addition, no bands other than those imputable to either

226   PNPase or S1 could be detected, thus suggesting that the two proteins do not form heteromeric

227   complexes on this RNA. We also measured PNPase- and S1-RNA affinity by EMSA using different

228   RNA probes covering different regions downstream the *pnp-p2* promoter. The results presented in Fig.

229   4C show that PNPase in all cases exhibits higher affinity than S1; moreover, both PNPase and S1 show

230   low affinity with probe PNPA101 (+1 to +101, which covers the primary RNase III stem; Kd = 5 and

231   44 nM for PNPase and S1, respectively) and the highest affinity with probe PNPD146, which covers

232   the +101 to + 247 region, downstream of the RNase III stem (Kd 1.6 and 22 nM, respectively; Fig. 4C).

233   Overall, these data indicate that PNPase and ribosomal protein S1 can bind competitively and

234   with differential affinity the 5'-UTR of *pnp* mRNA.

235

DISCUSSION

236

237

238   Both models for PNPase autogenous regulation proposed by Portier and collaborators (15, 16)

239 posit a two-step mechanism: first, RNase III creates the substrate for PNPase (14), which in turn

240 destabilizes the RNase III-processed *pnp* mRNA. In the former model, it was proposed that PNPase

241 induces the degradation of its RNase III processed messenger by preventing its translation (15). In the

242 later elegant model (16), PNPase controls its own expression by degrading the small RNA, generated

243 by RNase III cleavage, in the double-stranded structure that protects the 5'-end of the processed *pnp*

244 mRNA UTR. Within this model, it was shown that degradation of the protective small RNA by PNPase

245 directs the RNase III-processed *pnp* mRNA to an RNase E-dependent decay pathway and that PNPase

246 was not implicated in translational repression of the stem-less mRNA (17). On the other hand, some

247 previously published data suggest a more complex scenario. For instance, point mutations mapping in

248 the immediate proximity of the *pnp* Shine-Dalgarno region (and thus located more than 70 nt

249 downstream of the RNase II cut site) affect *pnp* autoregulation by reducing two- to threefold the extent

250 of repression by PNPase (see table II, strains GFX5311 and GFV5311; 14), a phenotype that is not easy

251 to reconcile with the current model of *pnp* autoregulation.

252   In this work, we show that another mechanism is involved in PNPase autoregulation. We found

253 that in presence of ectopically expressed PNPase, the repression of a *pnp-lacZ* translational fusion in an

254 *rnc⁻* strain is reduced to about a half of that obtained in the *rnc⁺* background but it is not abolished. This

255 clearly indicates that in addition to the RNase III-dependent pathway (RTD), an RNase III-independent

256 (RTI) pathway contributes to PNPase autogenous regulation. In agreement with an RTI pathway, in a

257 different *E. coli* strain and with a similar reporter system Robert-Le Meur and Portier (14) found a

258 twofold repression by PNPase expressed at the *pnp* chromosomal locus in an *rnc⁻* background (see in

259 Table IV, column pBPΔ7, ratio of the *rnc⁻ pnp⁻* GF494 and *rnc⁻ pnp⁺* GF493 strains). In contrast,

260 however, essentially no repression by PNPase expressed from a plasmid was found in the *rnc⁻ pnp⁻*

261 strain (Table IV, GF494 repression ratio 1.1). This discrepancy was not addressed.

262   Additional evidence for a PNPase-dependent, RTI pathway is provided by the observation that a

263 PNPase mutant lacking phosphorolytic activity but proficient in RNA binding partially regulates *pnp-*

264 *lacZ* expression both in the *rnc⁺* and in the *rnc⁻* backgrounds with similar efficiency, whereas,

265 consistently with previous data (25, 29, 30), PNPase mutants with defects in the RNA binding domains

266 could not. Thus, RTI pathway acts *via* RNA binding. Since the native *pnp* mRNA (not processed by

267 RNase III) is very stable also in the presence of PNPase and is intrinsically translatable (13, 17, 31), we

268 suggest that PNPase binding prevents its translation. This could reconcile evidence for translational

269 repression participating in PNPase autogenous regulation (14, 15) with the observation that PNPase is

270 not implicated in translational repression in the RTD pathway (17).

271   Point mutations or deletions of the RNA binding domains KH and/or S1 affect substrate affinity

272 (24, 26, 27, 32). Interestingly, a strong correlation between RNA affinity and autoregulation has been

273 observed (25). These data may fit the RTD model by implying that PNPase recruitment to the *pnp*

274 mRNA UTR is a limiting step in auto regulation. In addition, mutations in the RNA binding domains

275 may also reduce to different extents PNPase catalytic activity (24, 26, 27, 32), and this could reduce the

276 efficiency of degradation of the protecting small RNA. However, the RTI model provides an

277 additional, although not mutually exclusive, mechanism that may contribute to the above correlation, as

278 mutations impairing RNA binding are predicted to affect translational repression. It thus appears that

279 PNPase interaction with the 5'-UTR of its mRNA may have a dual effect: i) before RNase III

280 processing, PNPase binding inhibits translation. The RTI pathway is reversible, since the unprocessed

281 *pnp* primary transcript is very stable also in presence of PNPase (31); ii) upon RNase III processing,

282 PNPase activity degrades the small protective RNA and irreversibly directs the stem-less mRNA to the

283 RNase E-dependent degradation pathway.

284   The primary *pnp* transcript has been shown to be translatable whereas the mature mRNA, not

285 annealed with the protecting small RNA, appears not to be (13, 17, 31). Our data suggest that the

286 RNase III-processed mRNA annealed with the small RNA, before PNPase degrades it, is also

287 translatable. In fact, if translation from the *pnp* 5'-UTR would only occur before RNase III cleavage,

288 the downstream RTD step, although relevant for the control of *pnp* mRNA stability (13, 14), would be

289 nevertheless uninfluential on PNPase expression. Our data, on the contrary, show stronger repression

290 levels when both RTI and RTD steps are operating as compared with the RTI pathway only (compare i)

291 Pnp$^+$ and PnpS438A in the *rnc*$^+$ strain and ii) *rnc*$^+$ and *rnc*$^-$ with Pnp$^+$; Fig. 2). This supports the idea

292 that in the RTD pathway, PNPase may act by converting a translatable form of *pnp* mRNA (with a 5'-

293 end, RNase III truncated stem) into an untranslatable stem-less molecule, which would be quickly

294 degraded through an RNase E-dependent decay pathway.

295   We previously showed that PNPase and the ribosomal protein S1 are the two main proteins able

296 to bind the 5'-UTR of *pnp* mRNA (21). We thus suggest that inhibition of *pnp* mRNA translation in the

297 RTI pathway occurs *via* PNPase competition with S1 for RNA binding. Consistently with this

298 hypothesis, we observed *in vitro* that PNPase competes with and completely displaces S1 from the 5'-

299 UTR of *pnp* mRNA at a threefold lower concentration than the ribosomal protein (Fig. 4A). In

300 agreement with this observation PNPase exhibits a much higher affinity than S1 for the 5'-UTR of *pnp*

301 mRNA (Fig. 4B-D). This higher affinity may allow the PNPase to compete with the much more

302 abundant S1 protein (33) for the interaction with the *pnp* mRNA.

303   In conclusion, we have identified a novel, PNPase-dependent and RNase III-independent pathway

304 that contributes to PNPase autogenous regulation in *E. coli*. This RTI pathway, unlike RTD

305 autoregulation, is reversible and does not require the catalytic activity of the enzyme, as PNPase binds

306 to the native *pnp* mRNA and likely prevents its translation. PNPase thus plays a direct role in its

307 autogenous regulation before the primary transcripts become engaged in the downstream RTD branch.

308   As the activity of RNase III is downregulated in response to different stresses (34), it is possible

309 that the relative impact of the two PNPase autoregulation pathways may change in different

310 physiological conditions. The two sides of the autogenous regulation process highlight the interplay

311 between translation and RNA decay machineries in fine-tuning the expression of a pleiotropic gene.

312

313

317

318

319

320

REFERENCES

321

322

323 1. **Symmons MF, Williams MG, Luisi BF, Jones GH, Carpousis AJ.** 2002. Running rings

324   around RNA: a superfamily of phosphate-dependent RNases. Trends BiochemSci **27:**11-18.

325 2. **Wang G, Shimada E, Koehler CM, Teitell MA.** 2012. PNPASE and RNA trafficking into

326   mitochondria. Biochim Biophys Acta **1819:**998-1007.

327 3. **Deutscher MP, Reuven NB.** 1991. Enzymatic basis for hydrolytic versus phosphorolytic

328   mRNA degradation in *Escherichia coli* and *Bacillus subtilis* ProcNatlAcadSciUSA **88:**3277-

329   3280.

330 4. **Carzaniga T, Antoniani D, Dehò G, Briani F, Landini P.** 2012. The RNA processing enzyme

331   polynucleotide phosphorylase negatively controls biofilm formation by repressing poly-N-

332   acetylglucosamine (PNAG) production in *Escherichia coli* C. BMC Microbiol **12:**270.

333 5. **Cardenas PP, Carzaniga T, Zangrossi S, Briani F, Garcia-Tirado E, Dehò G, Alonso JC.**

334   2011. Polynucleotide phosphorylase exonuclease and polymerase activities on single-stranded

335   DNA ends are modulated by RecN, SsbA and RecA proteins. Nucleic Acids Res **39:**9250-9261.

336 6. **Piazza F, Zappone M, Sana M, Briani F, Dehò' G.** 1996. Polynucleotide phosphorylase of

337   *Escherichia coli* is required for the establishment of bacteriophage P4 immunity. JBacteriol

338   **178:**5513-5521.

339 7. **Zangrossi S, Briani F, Ghisotti D, Regonesi ME, Tortora P, Dehò' G.** 2000. Transcriptional

340   and post-transcriptional control of polynucleotide phosphorylase during cold acclimation in

341   *Escherichia coli.* MolMicrobiol **36:**1470-1480.

342 8. **Wu J, Jiang Z, Liu M, Gong X, Wu S, Burns CM, Li Z.** 2009. Polynucleotide phosphorylase

343   protects *Escherichia coli* against oxidative stress. Biochemistry **48:**2012-2020.

344 9. **Takata R, Mukai T, Hori K.** 1985. Attenuation and processing of RNA from the *rpsO-pnp*

345   transcription unit of *Escherichia coli.* Nucleic Acids Res **13:**7289-7297.

346 10. **Régnier P, Portier C.** 1986. Initiation, attenuation and RNase III processing of transcripts from

347 the *Escherichia coli* operon encoding ribosomal protein S15 and polynucleotide phosphorylase.

348 JMolBiol **187:**23-32.

349 11. **Régnier P, Grunberg-Manago M.** 1989. Cleavage by RNase III in the transcripts of the *met Y-*

350 *nus-A-infB* operon of *Escherichia coli* releases the tRNA and initiates the decay of the

351 downstream mRNA. JMolBiol **210:**293-302.

352 12. **Portier C, Régnier P.** 1984. Expression of the *rpsO* and *pnp* genes: structural analysis of a

353 DNA fragment carrying their control regions. Nucleic Acids Res **12:**6091-6102.

354 13. **Takata R, Mukai T, Hori K.** 1987. RNA processing by RNase III is involved in the synthesis

355 of *Escherichia coli* polynucleotide phosphorylase. MolGenGenet **209:**28-32.

356 14. **Robert-Le Meur M, Portier C.** 1992. *E. coli* polynucleotide phosphorylase expression is

357 autoregulated through an RNase III-dependent mechanism. EMBO J **11:**2633-2641.

358 15. **Robert-Le Meur M, Portier C.** 1994. Polynucleotide phosphorylase of *Escherichia coli*

359 induces the degradation of its RNase III processed messenger by preventing its translation.

360 Nucleic Acids Res **22:**397-403.

361 16. **Jarrige AC, Mathy N, Portier C.** 2001. PNPase autocontrols its expression by degrading a

362 double-stranded structure in the *pnp* mRNA leader. EMBO J **20:**6845-6855.

363 17. **Carzaniga T, Briani F, Zangrossi S, Merlino G, Marchi P, Dehò G.** 2009. Autogenous

364 regulation of *Escherichia coli* polynucleotide phosphorylase expression revisited. JBacteriol

365 **191:**1738-1748.

366 18. **Ghisotti D, Chiaramonte R, Forti F, Zangrossi S, Sironi G, Dehò' G.** 1992. Genetic analysis

367 of the immunity region of phage-plasmid P4. MolMicrobiol **6:**3405-3413.

368   19.   **Carzaniga T, Mazzantini E, Nardini M, Regonesi ME, Greco C, Briani F, De Gioia L,**

369   **Dehò G, Tortora P.** 2014. A conserved loop in polynucleotide phosphorylase (PNPase)

370   essential for both RNA and ADP/phosphate binding. Biochimie **97:**49-59.

371   20.   **Fontanella L, Pozzuolo S, Costanzo A, Favaro R, Dehò' G, Tortora P.** 1999. Photometric

372   assay for polynucleotide phosphorylase. AnalBiochem **269:**353-358.

373   21.   **Briani F, Curti S, Rossi F, Carzaniga T, Mauri P, Dehò G.** 2008. Polynucleotide

374   phosphorylase hinders mRNA degradation upon ribosomal protein S1 overexpression in

375   *Escherichia coli.* RNA **14:**2417-2429.

376   22.   **Delvillani F, Papiani G, Dehò G, Briani F.** 2011. S1 ribosomal protein and the interplay

377   between translation and mRNA decay. Nucleic Acids Res **39:**7702-7715.

378   23.   **Charollais J, Pflieger D, Vinh J, Dreyfus M, Iost I.** 2003. The DEAD-box RNA helicase

379   SrmB is involved in the assembly of 50S ribosomal subunits in *Escherichia coli.* MolMicrobiol

380   **48:**1253-1265.

381   24.   **Matus-Ortega ME, Regonesi ME, Pina-Escobedo A, Tortora P, Dehò G, Garcia-Mena J.**

382   2007. The KH and S1 domains of *Escherichia coli* polynucleotide phosphorylase are necessary

383   for autoregulation and growth at low temperature. Biochimica et Biophysica Acta-Gene

384   Structure and Expression **1769:**194-203.

385   25.   **Wong AG, McBurney KL, Thompson KJ, Stickney LM, Mackie GA.** 2013. S1 and KH

386   domains of polynucleotide phosphorylase determine the efficiency of RNA binding and

387   autoregulation. J Bacteriol **195:**2021-2031.

388   26.   **Stickney LM, Hankins JS, Miao X, Mackie GA.** 2005. Function of the conserved S1 and KH

389   domains in polynucleotide phosphorylase. JBacteriol **187:**7214-7221.

390 27. **Briani F, Del Favero M, Capizzuto R, Consonni C, Zangrossi S, Greco C, De Gioia L,**

391 **Tortora P, Dehò G.** 2007. Genetic analysis of polynucleotide phosphorylase structure and

392 functions. Biochimie **89:**145-157.

393 28. **Xu F, Cohen SN.** 1995. RNA degradation in *Escherichia coli* regulated by 3' adenylation and 5'

394 phosphorylation. Nature **374:**180-183.

395 29. **Garcia-Mena J, Das A, Sanchez-Trujillo A, Portier C, Montanez C.** 1999. A novel mutation

396 in the KH domain of polynucleotide phosphorylase affects autoregulation and mRNA decay in

397 *Escherichia coli.* MolMicrobiol **33:**235-248.

398 30. **Fernandez-Ramirez F, Bermudez-Cruz RM, Montanez C.** 2010. Nucleic acid and protein

399 factors involved in *Escherichia coli* polynucleotide phosphorylase function on RNA. Biochimie

400 **92:**445-454.

401 31. **Portier C, Dondon L, Grunberg-Manago M, Régnier P.** 1987. The first step in the functional

402 inactivation of the *Escherichia coli* polynucleotide phosphorylase messenger is a ribonuclease

403 III processing at the 5' end. EMBO J **6:**2165-2170.

404 32. **Jarrige A, Brechemier-Baey D, Mathy N, Duche O, Portier C.** 2002. Mutational analysis of

405 polynucleotide phosphorylase from *Escherichia coli.* JMolBiol **321:**397-409.

406 33. **Ishihama Y, Schmidt T, Rappsilber J, Mann M, Hartl FU, Kerner MJ, Frishman D.** 2008.

407 Protein abundance profiling of the *Escherichia coli* cytosol. BMC Genomics **9:**102.

408 34. **Kim KS, Manasherob R, Cohen SN.** 2008. YmdB: a stress-responsive ribonuclease-binding

409 regulator of *E. coli* RNase III activity. Genes Dev **22:**3497-3508.

410 35. **Sasaki I, Bertani G.** 1965. Growth abnormalities in Hfr derivatives of *Escherichia coli* strain

411 C. JGenMicrobiol **40:**365-376.

412 36. **Regonesi ME, Del Favero M, Basilico F, Briani F, Benazzi L, Tortora P, Mauri P, Dehò'**
413   **G.** 2006. Analysis of the *Escherichia coli* RNA degradosome composition by a proteomic
414   approach. Biochimie **88:**151-161.

415 37. **Grant SG, Jessee J, Bloom FR, Hanahan D.** 1990. Differential plasmid rescue from
416   transgenic mouse DNAs into *Escherichia coli* methylation-restriction mutants. Proc Natl Acad
417   Sci U S A **87:**4645-4649.

418 38. **Regonesi ME, Briani F, Ghetta A, Zangrossi S, Ghisotti D, Tortora P, Dehò' G.** 2004. A
419   mutation in polynucleotide phosphorylase from *Escherichia coli* impairing RNA binding and
420   degradosome stability. Nucleic Acids Res **32:**1006-1017.

421 39. **Guzman LM, Belin D, Carson MJ, Beckwith J.** 1995. Tight regulation, modulation, and
422   high-level expression by vectors containing the arabinose PBAD promoter. JBacteriol
423   **177:**4121-4130.

424 40. **Wall JD, Harriman PD.** 1974. Phage P1 mutants with altered transducing abilities for
425   *Escherichia coli*. Virology **59:**532-544.

426
427

428
429

TABLES

TABLE 1. Bacteria, plasmids and phages.

Strain	Relevant characters[a]	Source/Reference
Bacteria		
C-1a	*E. coli* C, prototrophic	(35)
C-5684	Δ*rnc38*::*kan*	(17)
C-5691	Δ*pnp751*	(36)
C-5691 (λGF2)	Δ*pnp751* λ *pnp-lacZ*	from C-5691 by lysogenization with λGF2 at 37 °C
C-5979	Δ*pnp751* Δ*rnc38*::*kan*	from C-5691 by P1HFT*C5684 transduction
C-5979 (λGF2)	Δ*pnp751* Δ*rnc38*::*kan* λ *pnp-lacZ*	by lysogenization with λGF2 at 37 °C
DH10B	Recipient strain for transformation by electroporation with new plasmid constructs	(37)
GF5322	*recA*::Tn*10 pnp*::Tn*5* (λ *pnp-lacZ*)	(14)
Plasmids		
pAZ101	pGZ119HE-*pnp*⁺; Cam^R	(38)
pAZ1112	pAZ101-*pnp*-S438A; Cam^R	(19)
pAZ133	pAZ101-*pnp*-ΔKH-S1 (*pnp*-833); Cam^R	(27)
pBAD24	*araC araBp*, ColE1; Amp^R	(39)
pBAD-pnp	pBAD24 *pnp-his*; Amp^R	(4)
pBAD-Pnp⁺	pBAD24 *pnp*⁺; Amp^R	BsiWI-HindIII fragment of pAZ101 cloned in pBAD-pnp
pBAD-pnpS438A	pBAD24 *pnp*-S438A; Amp^R	BsiWI-HindIII fragment of pAZ1112 cloned in pBAD-pnp

pBAD-pnpΔKHS1	pBAD24 *pnp*-ΔKH-S1; Amp^R	BsiWI-HindIII fragment of pAZ133 cloned in pBAD-pnp

Phages		
P1HFT	high frequency of transduction	(40) *via* R. Calendar
λGF2	λ *pnp-lacZ* translational fusion from GF5322	(14)

434

435

436

437   TABLE 2. Oligonucleotides[a]

438

Number	5′→3′ sequence	Template for[b]	Coordinates[c]
FG0676[d]	**CTAATACGACTCACTATAGGG** ATGAATGATCTTCCGTTGC	PNPA247; PNPA157; PNPA101	3311326-3311308
FG0678	CAGCGGCAGTAGCCTGACGAGC	PNPA247; PNPD146	3311078-3311099
FG1387	AATGTAATATCCTTTCTCTTTCTTAG	PNPA157	3311167-3311192
FG1625[d]	**CTAATACGACTCACTATAGGG** GGGTATTAACACCAGTGCCG	PNPD146	3311223-3311204
FG1710	GATCTTCTGCGCATCCTCGC	PNPA101	3311224-3311243

439

440   [a] Used as PCR primers with pAZ101 DNA as a template

441   [b] The PCR products were used as T7 RNA polymerase template to obtain the RNA probes indicated

442   [c] Co-ordinates are referred to NCBI Accession Number U00096.2.

443   [d] Boldface letters correspond to T7 promoter sequence.

444

445

446

447   **FIGURE LEGENDS**

448

449   **FIG 1** Genetic organization of the *E. coli pnp* regulatory region. Upper scale corresponds to the

450   MG1655 reverse genomic sequence 3,309,850-3,309,100 (EMBL Accession No. AE000397), lower

451   scale refers to the transcript from P2 promoter. P1, P2; promoters; t1: transcription terminator; $RIII_1$,

452      $RIII_2$: RNase III cut sites; arrows in the lower part represent the RNA probes used in this study.

453

454   **FIG 2** RNase III-independent PNPase autogenous regulation. β-galactosidase activity expressed from

455   *pnp-lacZ* translational fusion. Cultures of strains C-5691 (λGF2), a Δ*pnp751* lysogenic for λ harbouring

456   an *pnp-lacZ* operon fusion and its Δ*rnc38*::*kan* derivative harbouring pBAD24 (empty vector), pBAD-

457   Pnp$^+$, pBAD-PnpS438A, or pBAD-PnpΔKHS1 were grown in LD with either arabinose or glucose to

458   induce or repress transcription of the cloned *pnp* allele, respectively. Culture samples were assayed for

459   β-galactosidase activity expressed from *pnp-lacZ* translational fusion of prophage λGF2, as detailed in

460   Materials and Methods. The histogram reports specific activity (S.A.) as nmoles of 2-nitrophenyl-β-D-

461   galactopyranoside converted to o-nitrophenol/min/mg of proteins. Repression Factor is the ratio of β-

462   galactosidase S.A. in cultures with not induced (empty bars) and induced (grey bars) PNPase.

463

464   **FIG 3** RNA binding by PNPase mutants. (A) PNPase- RNA UV-cross linking in crude cell extracts.

465   Crude cell extracts (0.4 μg) of strains listed in legend of FIG2 grown in LD arabinose to induce

466   transcription of the cloned *pnp* allele were incubated with 100,000 cpm of [^{32}P] uniformly labeled

467   PNPA247 RNA probe (1 nM) and the samples were UV irradiated (254 nm, 2.8 J cm^{-2}). The reaction

468   products were then digested with RNase A, fractionated by 10% SDS-PAGE and visualized by

469   phosphorimaging (upper panel) or western blotted with α-PNPase antibodies (lower panel). The bands

470   in the controls lacking PNPase correspond to S1 ribosomal protein (27). The figures below the lanes

471   refer to PNPase binding efficiency. Signal intensity of each sample from (A) was quantified by

472   ImageQuant and normalized to the wild type PNPase signal. Binding efficiency is given as the ratio of

473   cross linking and western blotting normalized signals. (B) S1-PNPase interaction. Crude extract of

474   strains expressing either wild-type PNPase (+) or the PnpΔKHS1 variant were incubated with S1-

475   coated magnetic beads. When indicated (RNase A +), the extract were pre-treated with RNase A to

476   degrade bulk mRNA. After incubation of the beads with the extracts and washing, S1 (with interacting

477   proteins and RNA) was eluted as detailed in Materials and Methods. Proteins in different fractions were

478   separated by SDS-PAGE and either blotted on a nitrocellulose filter and immunodecorated with

479   PNPase specific antiserum (upper panel) or silver stained (lower panel). 10 µl aliquots of each fraction

480   were loaded on the gel for silver staining, whereas 1 µl (FT, W1 and W2) or 10 µl (E) were analysed by

481   western blotting. FT, crude extract after incubation with S1 coated beads; W1, first wash; W2, second

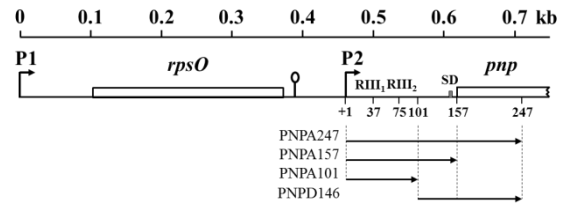482   wash; E, proteins co-eluting with S1.

483

484   **FIG 4** PNPase and S1 binding to the *pnp* mRNA leader region. (A) PNPase-S1 competitive cross-

485   linking for *pnp* mRNA leader. 100,000 cpm uniformly labelled PNPA157 probe (0.6 nM) was

486   incubated 20 min at 21 °C with 30 nM S1 and increasing (0, 1, 3, 6, 9, 12 nM) concentrations of

487   PNPase. The samples were then UV irradiated (254 nm, 2.8 J cm^{-2}), digested with RNase A and

488   fractionated by SDS-PAGE. (B) and (C) PNPase and S1 binding to different regions of *pnp* mRNA

489   leader. EMSA was performed as described in Materials and Methods using [^{32}P]-5'-end-labeled

490   PNPA101 (14,000 cpm, 0.5 nM) or PNPD146 (30,000 cpm, 0.5 nM) probes incubated 20 min at 21 °C

491   with increasing concentrations of PNPase (0, 0.5, 1, 2, 4, 8 nM) or S1 (0, 2, 4, 12, 36, 72 nM). The

492   unbound probe band intensities were evaluated by ImageQuant, normalized to the intensity of the 0 nM

493   PNPase or S1 sample and plotted versus PNPase or S1 concentration; dissociation constant (K_d) was

494   evaluated as the PNPase or S1 concentration giving 50% probe binding. A plot is shown as an example

495   on the right of the western blot image in (B), whereas K_d is indicated on the bottom of each panel. U,

496   unbound probe. The stars in (B) indicate signals likely due to alternative conformations of the unbound
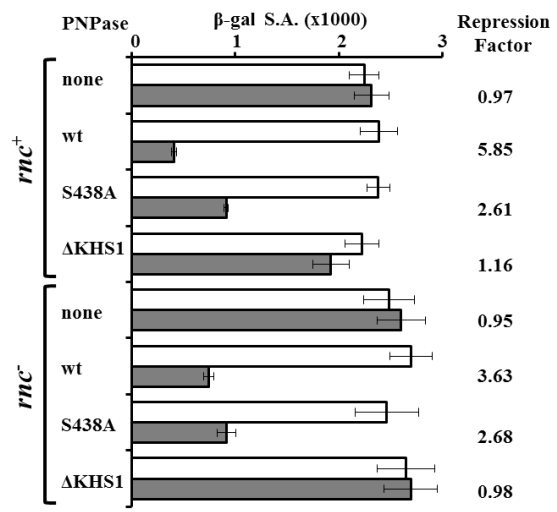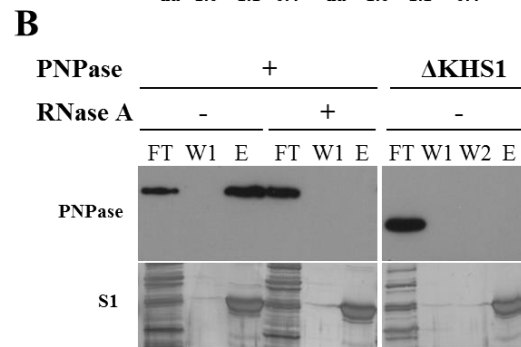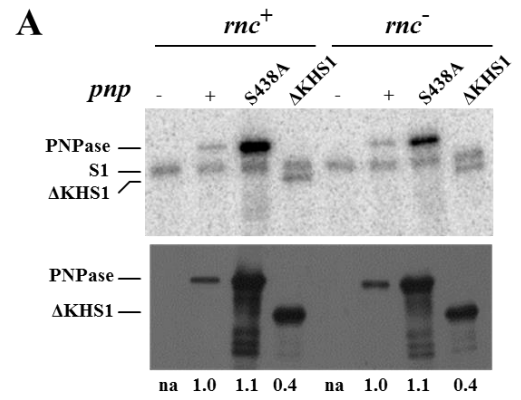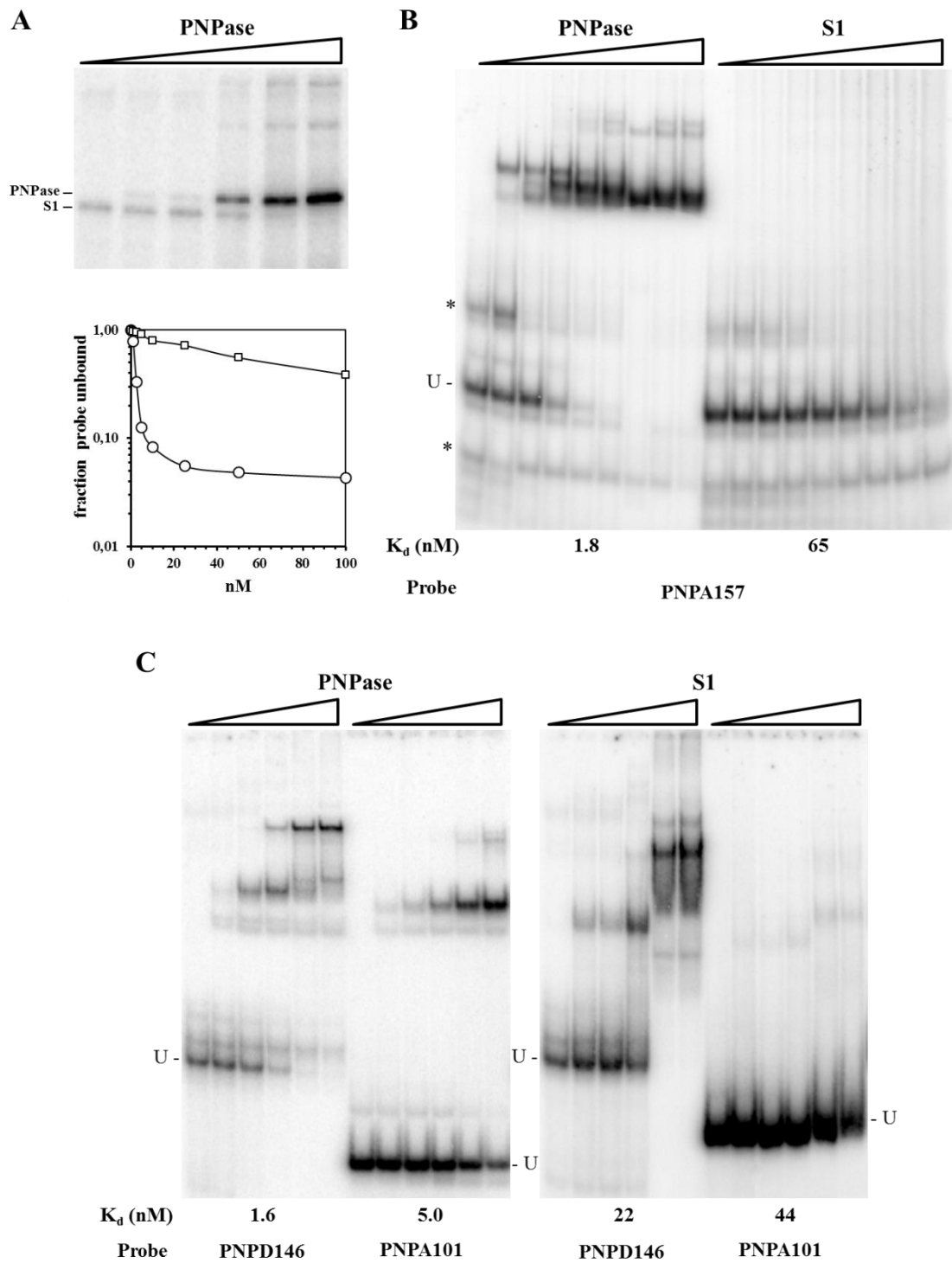
497   probe.

498

499

500

FIG 1

FIG 2

FIG 3

A

PNPase

PNPase —
S1 —

fraction probe unbound

nM

B

PNPase   S1

*

U -

*

K_d (nM)   1.8   65

Probe   PNPA157

C

PNPase   S1

U -   U -

- U

- U

K_d (nM)   1.6   5.0   22   44

Probe   PNPD146   PNPA101   PNPD146   PNPA101

Fig 4